R-matrix

Nigel Badnell

Department of Physics
University of Strathclyde
Glasgow, UK

Overview

- R-matrix method
- Parallel codes
- R-matrix with pseudo-states (RMPS)
- Intermediate coupling frame transformation (ICFT) R-matrix
- Dirac R-matrix
- Future thoughts

Motivation

Q. Why atomic collisions?

A. Spectroscopic diagnostic modelling of non-LTE astrophysical and laboratory plasmas.

Simplest model: excited states of an atom/ion are populated by collisional excitation and de-populated by radiative transitions.

So, need excitation rate coefficients — Maxwellian average of excitation cross sections.

A typical cross section?

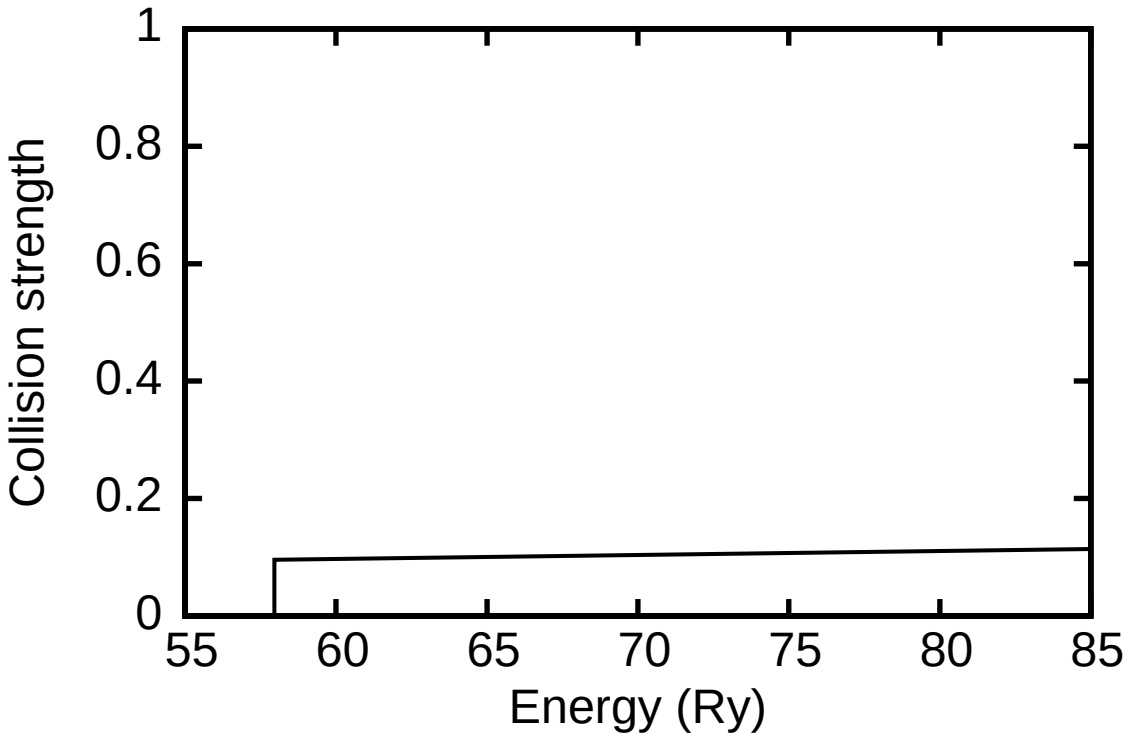

(Collision strength $\Omega = \omega k^2 \sigma / \pi a_0^2$.)

No!

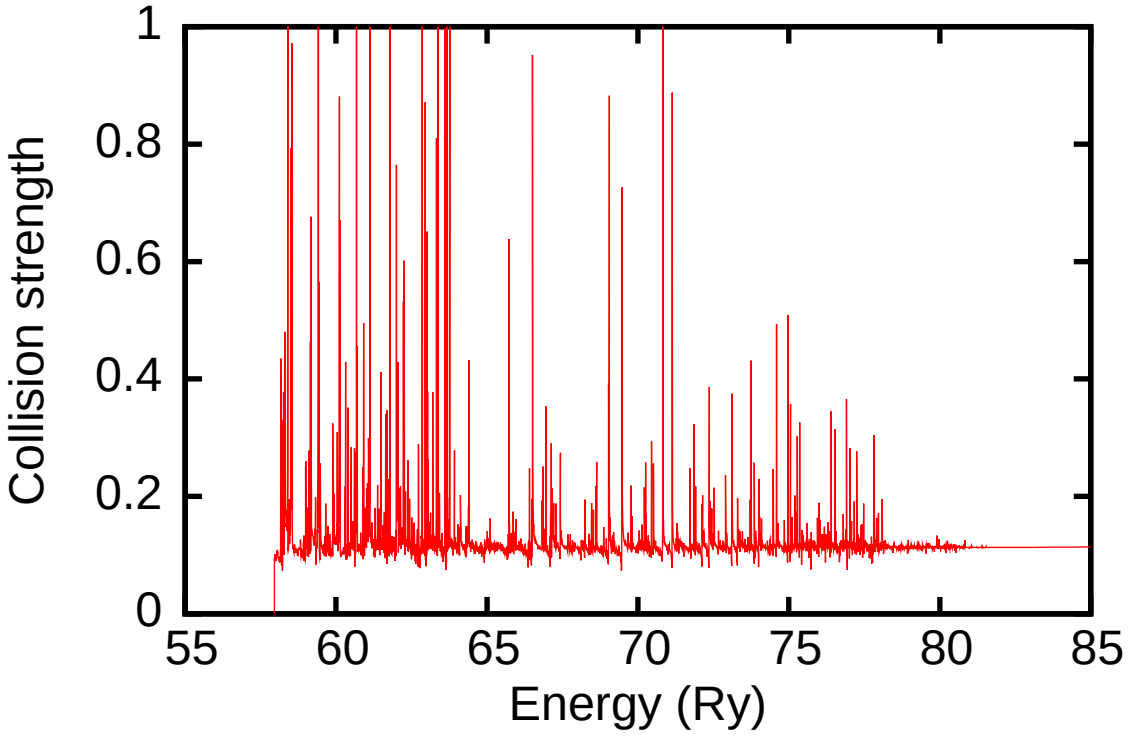

(129CC Dirac–Coulomb R-matrix collision strength for the $3\mathrm{d}^{10}\ {}^1\mathrm{S}_0 - 4\mathrm{d}^1\mathrm{S}_0$ transition in Xe^{26+}.)

The difference!

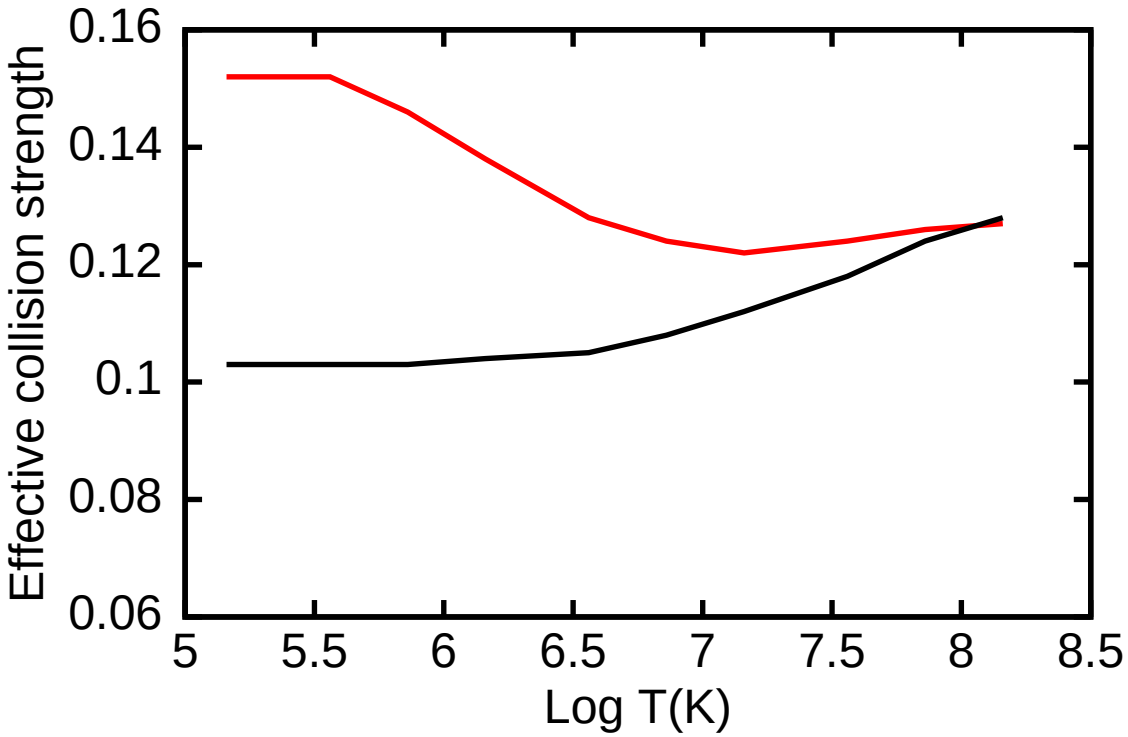

(Effective (Maxwell-averaged) collision strength $\Upsilon = (kT)^{1/2}\omega q/(2\alpha c a_0^2\sqrt{\pi})$.)

Basic Scattering Theory (in one page)

Write the (anti-symmetric) total wavefunction for the atom-colliding particle system as

$$\Psi = A\sum\!\!\!\!\!\!\int_{\nu} \psi_\nu \phi \,, \tag{1}$$

where the ψ_ν form a complete set of atomic eigenstates (discrete plus continuous).Then solve for ϕ from

$$H\Psi = E\Psi \,, \tag{2}$$

where H and E are the total Hamiltonian and Energy of the system, respectively. The difference between the large distance asymptotic wavefunction for the colliding particle (ϕ) and that of a plane (or Coulomb) wave leads to the probability of scattering (by a non-Coulomb potential) that has taken place — the S- or scattering matrix, of reactions between initial and final atomic states. A more useful quantity, simply related to the S-matrix, is the cross section, σ.

The Solution

Use of (1) and (2) leads to an infinite set of coupled integro-differential equations (integro because the exchange operator is a non-local). By discretizing the continuum we can form a quadrature for (1) and reduce (2) to a finite-set of close-coupling (CC) equations. Historically, only a few low-lying states of direct interest were included in the CC equations.

In (1) we assumed that we had all atomic eigenstates to any required level of accuracy. In practice, determining a sufficiently accurate atomic structure, while keeping the CC expansion manageable, is a significant issue for any collision calculation.

The wavefunction for the colliding particle (ϕ) is also expanded as an infinite sum of partial waves (angular momentum states). Typically, ≤ 10 angular momentum states couple to a given target state so as to give the same, conserved, total angular momentum for the combined system.

So, given a set of coupled integro-differential equations, how do we best go about solving them, given the complex resonance structure that we must resolve?

The R-matrix Method

The approach of the R-matrix method (Burke & Robb, 1975) to scattering builds upon the idea of dividing-up configuration space into two regions, an inner one where the scattering potential is non-trivial and the scattering wavefunction complicated, and an outer region where the potential is 'simple', for example, it vanishes or is Coulombic, and the radial function is represented by its asymptotic form, viz.

$$f_l(r) = f_l^a(r), \tag{3}$$

for $r \geq r_0$, the R-matrix boundary.

For example, a partial plane wave equation

$$\left(\frac{\mathrm{d}^2}{\mathrm{d}r^2} - \frac{l(l+1)}{r^2} + k^2 \right) f_l^a(r) = 0 \tag{4}$$

with general solution

$$f_l^a(r) = A_l \left[s_l(kr) + K_l c_l(kr) \right] \tag{5}$$

and $K_l = \tan \delta_l$, where δ_l is the phase shift and A_l is a normalization constant.

We denote the two independent real solutions by $s_l(kr)$ and $c_l(kr)$ (the so-called s and c functions). These are related to the spherical Bessel and Neumann functions $j_l(x)$ and $n_l(x)$ via

$$s_l(x) = x j_l(x) \tag{6}$$

and

$$c_l(x) = -x n_l(x). \tag{7}$$

Asymptotically,

$$s_l(x) \underset{x \to \infty}{\sim} \sin\left(x - \frac{l\pi}{2} \right) \tag{8}$$

$$c_l(x) \underset{x \to \infty}{\sim} \cos\left(x - \frac{l\pi}{2} \right). \tag{9}$$

In the inner-region ($r \leq r_0$) we denote the regular solution satisfying $f_l(r = 0) = 0$

by $f_l^b(r)$, i.e.

$$f_l(r) = f_l^b(r) \tag{10}$$

for $r \leq r_0$.

We can determine K_l (and hence σ_l) from $f_l^b(r)$ by matching logarithmic derivatives at the boundary $r = r_0$.

So, define

$$\gamma \equiv \left[\frac{\mathrm{d}f_l^b}{\mathrm{d}r}\frac{1}{f_l^b}\right]_{r=r_0} = \left[\frac{\mathrm{d}f_l^a}{\mathrm{d}r}\frac{1}{f_l^a}\right]_{r=r_0}. \tag{11}$$

Substituting for f_l^a, $f_l^{a\prime}$ from (5) we have

$$K_l = \tan\delta_l = \frac{s_l'(kr_0) - \gamma s_l(kr_0)}{\gamma c_l(kr_0) - c_l'(kr_0)}, \tag{12}$$

where the value of γ is given by the logarithmic derivative of f_l^b. We thus require to

determine f_l^b. For $l = 0$, $s_0 = \sin$ and $c_0 = \cos$ and

$$K_0 = \tan \delta_0 = \frac{k \cos(kr_0) - \gamma \sin(kr_0)}{\gamma \cos(kr_0) + k \sin(kr_0)}. \tag{13}$$

Since $f_l^b(r)$ is required only over a finite range, $0 \leq r \leq r_0$, we can approximate it by a suitable linear combination of convenient basis functions $u_i(r)$. Thus,

$$f_l^b(r) = \sum_{i=0}^{\infty} a_i u_i(r). \tag{14}$$

The coefficients a_i are determined by requiring that $f_l^b(r)$ satisfies

$$\left(\frac{\mathrm{d}^2}{\mathrm{d}r^2} - \frac{l(l+1)}{r^2} - V(r) + k^2 \right) f_l^b(r) = 0 \tag{15}$$

still, at least to a certain level of accuracy.

Various alternatives are possible. The Wigner–Eisenbud method is one of the most

commonly used in atomic physics. We illustrate the case of $l = 0$. Then, we have that

$$\left(\frac{\mathrm{d}^2}{\mathrm{d}r^2} - V(r) \right) u_i(r) = -k_i^2 u_i(r), \tag{16}$$

for $i = 1, 2, \ldots \infty$, over $0 \leq r \leq r_0$, subject to the boundary conditions

$$u_i(0) = 0 \tag{17}$$

and

$$\left[\frac{\mathrm{d}u_i}{\mathrm{d}r} \frac{1}{u_i} \right]_{r=r_0} = b, \tag{18}$$

where b is a fixed (which characterizes Wigner–Eisenbud) arbitrary number.

The boundary condition (18) results in a discrete e-value spectrum $\{k_i^2 : i = 1, 2, \ldots \infty\}$.

Note,

$$\int_0^{r_0} u_i u_j \mathrm{d}r = \delta_{ij}, \tag{19}$$

for $i, j = 1, 2, \ldots \infty$, on renormalizing the u_i.

With

$$f_0^b(r) = \sum_{i=1}^{\infty} a_i u_i(r) \tag{20}$$

then

$$a_i = \int_0^{r_0} u_i(r) f_0^b(r) \mathrm{d}r. \tag{21}$$

By multiplying (15) by $u_i(r)$ and (16) by $f_0^b(r)$, subtracting and integrating over r, we have

$$\int_0^{r_0} \mathrm{d}r \left(f_0^b \frac{\mathrm{d}^2 u_i}{\mathrm{d}r^2} - u_i \frac{\mathrm{d}^2 f_0^b}{\mathrm{d}r^2} \right) = (k^2 - k_i^2) \int_0^{r_0} u_i f_0^b \mathrm{d}r. \tag{22}$$

On integrating by parts, we obtain

$$\left[f_0^b \frac{\mathrm{d}u_i}{\mathrm{d}r} - u_i \frac{\mathrm{d}f_0^b}{\mathrm{d}r} \right]_{r=r_0} = (k^2 - k_i^2) a_i, \tag{23}$$

which determines the a_i.

At $r = r_0$,

$$f_0^b(r_0) = \sum_{i=1}^{\infty} a_i u_i(r_0) \tag{24}$$

$$= \sum_{i=1}^{\infty} \frac{u_i(r_0)}{k^2 - k_i^2} \left[f_0^b \frac{\mathrm{d}u_i}{\mathrm{d}r} - u_i \frac{\mathrm{d}f_0^b}{\mathrm{d}r} \right]_{r=r_0} . \tag{25}$$

On substituting for the logarithmic derivative γ (11) into (25), and using our boundary condition (18), we have

$$\gamma = b + \frac{1}{R} \tag{26}$$

where the R-matrix, R, is defined by

$$R \equiv \sum_{i=1}^{\infty} \frac{[u_i(r_0)]^2}{k_i^2 - k^2}. \tag{27}$$

Determination of R then enables $K_0 = \tan\delta_0$ to be determined from (via γ)

$$K_0 = \frac{-\sin(kr_0) + R(k\cos(kr_0) - b\sin(kr_0))}{\cos(kr_0) + R(k\sin(kr_0) + b\cos(kr_0))}. \tag{28}$$

Generalization to non-zero angular momentum ($l > 0$) and the Coulomb potential in the external region is straightforward (see Burke & Robb, 1975).

We note that the R-matrix consists of a series of poles along the real k^2 axis. If k^2 is near one of the poles k_i^2, then $R(k^2)$ can be approximated by a single term,

$$R(k^2) \approx \frac{\left[u_i(r_0)\right]^2}{k_i^2 - k^2}. \tag{29}$$

Even if the original potential satisfied by $f_l(r)$ is the same one used to determine the $u_i(r)$, there is still an advantage since we need only solve it a small number of times to determine the basis functions but can then determine the scattering cross section at the very large number of energies necessary to resolve resonance structure. Furthermore, if we

choose a basis set v_i^0 which is easily evaluated, say

$$\left(\frac{\mathrm{d}^2}{\mathrm{d}r^2} + V_0(r) + k_{0i}^2\right) v_i^0 = 0. \tag{30}$$

Then, if we approximate the first N e-solutions u_i, for $i = 1, 2, \ldots N$, by

$$u_i \approx v_i^{(N)} = \sum_{i'=1}^{N} c_{i'i}^{(N)} v_{i'}^0, \tag{31}$$

we can expand

$$f_0^{b(N)}(r) = \sum_{i=1}^{N} a_i^{(N)} v_i^{(N)}, \tag{32}$$

where $f_0^{b(N)}(r)$ is an approximate solution to the exact solution $f_0^b(r)$ at k^2. Then

$$R^{(N)} = \sum_{i=1}^{N} \frac{\left[v_i^{(N)}(r_0)\right]^2}{k_i^{(N)2} - k^2}, \tag{33}$$

where $k_i^{(N)2} \geq k_i^2$, for $i = 1, 2, \ldots N$ and $k_i^{(N)2}$ and $c_{i'i}^{(N)}$ are determined by diagonalizing

$$L_{ii'}^{(N)} = -\int_0^{r_0} v_i^0 \left(\frac{\mathrm{d}^2}{\mathrm{d}r^2} + V(r) \right) v_{i'}^0 \mathrm{d}r, \tag{34}$$

for $i, i' = 1, 2, \ldots N$, i.e.

$$\mathbf{c}^{(N)\mathrm{T}} \cdot \mathbf{L}^{(N)} \cdot \mathbf{c}^{(N)} = \left[\mathbf{k}^{(N)} \right]^2 = \mathrm{diag} \left(k_i^{(N)2} \right). \tag{35}$$

Thus, we only require to converge the sum over N. The rate of convergence can be improved by correcting for the effect of higher poles: $N+1, \ldots \infty$ — this is the *Buttle correction*:

Solve for $v^0(r)$ at a *non-pole* energy k^2. Then, from (26)

$$R^0 = [\gamma - b]_{r=r_0}^{-1} = v^0(r_0) \left[\frac{\mathrm{d}v^0(r)}{\mathrm{d}r} - b v^0(r) \right]_{r=r_0}^{-1}. \tag{36}$$

The Buttle correction, R^c, is given by

$$R^c = R^0 - \sum_{i=1}^{N} \frac{\left[v_i^0(r_0)\right]^2}{k_{0i}^2 - k^2}. \tag{37}$$

Then, the Buttle-corrected R-matrix is given by

$$R = R^{(N)} + R^c, \tag{38}$$

i.e. the high poles ($> N$) are approximated by the zero order basis.

The power of the R-matrix method lies with the fact that we have replaced solving complex multi-channel coupled integro-differential equations (in the general scattering case) by a small set of uncoupled ordinary differential equations (the potential V_0 can be fairly crude) and a matrix diagonalization (34). This diagonalization has to be carried-out only ONCE to enable the R-matrix to be determined at ALL energies. This is of enormous importance for the low-energy cross sections which are dominated by narrow resonance structures and require a solution at $\sim 10^4$ energies.

The main drawback to the R-matrix method is that it does not scale well to 'high' energies. To determine the R-matrix and, hence, cross section at k^2, say, requires N to be sufficiently large so that the highest few basis energies k_i^2 satisfy $k_i^2 > k^2$. Typically, it is only practical to work with $N = 20 - 50$ as matrix diagonalization is an $N_{\rm r}^3$ process, where $N_{\rm r}$ is the rank of the matrix. Here $N_{\rm r} = N \times N_{\rm c}$ where $N_{\rm c}$ is the number of scattering channels required to describe the problem. In a complex atom the number of channels increases rapidly. The current practical limit utilizing massively parallel machines (e.g. 5000 processors) is a rank of $N_{\rm r} \approx 150,000$. We also require to carry out this diagonalization ≈ 100 times (so as to converge the partial wave expansion).

However, we only need solve the scattering problem with the R-matrix method up to a few times the ionization energy of the atom so as to establish its high energy behaviour. This is then easily connected to its infinite energy solution, which is identical to that of a (maybe relativistic) plane wave.

Outer Region Solutions

We have gone into the solution of the collision problem in the inner region in some detail. But, as noted, this must be matched to the outer region solution for us to be able to extract the scattering probability etc. In the outer region we have, maybe, a Coulomb potential plus long-range multipole potentials ($1/r^{\lambda+1}, \lambda \geq 1$).

Solution in the outer region is computationally non-trivial — the coupled differential equations need to be solved at every energy, maybe several tens of thousands. We initially solve the uncoupled Coulomb (or plane wave) problem and treat the long-range multipole potentials as a perturbation. We can also factor-out much of the strong energy dependence of the scattering matrices, and so interpolate them as a function of energy — multi-channel quantum defect theory. Even so, it is common for the outer region problem to take more computer time than the inner region.

Both regions are amenable to massively parallel calculations — matrix diagonalization via scaLAPACK, while the outer region solution is embarrassingly parallel by energy.

Code Suite Overview

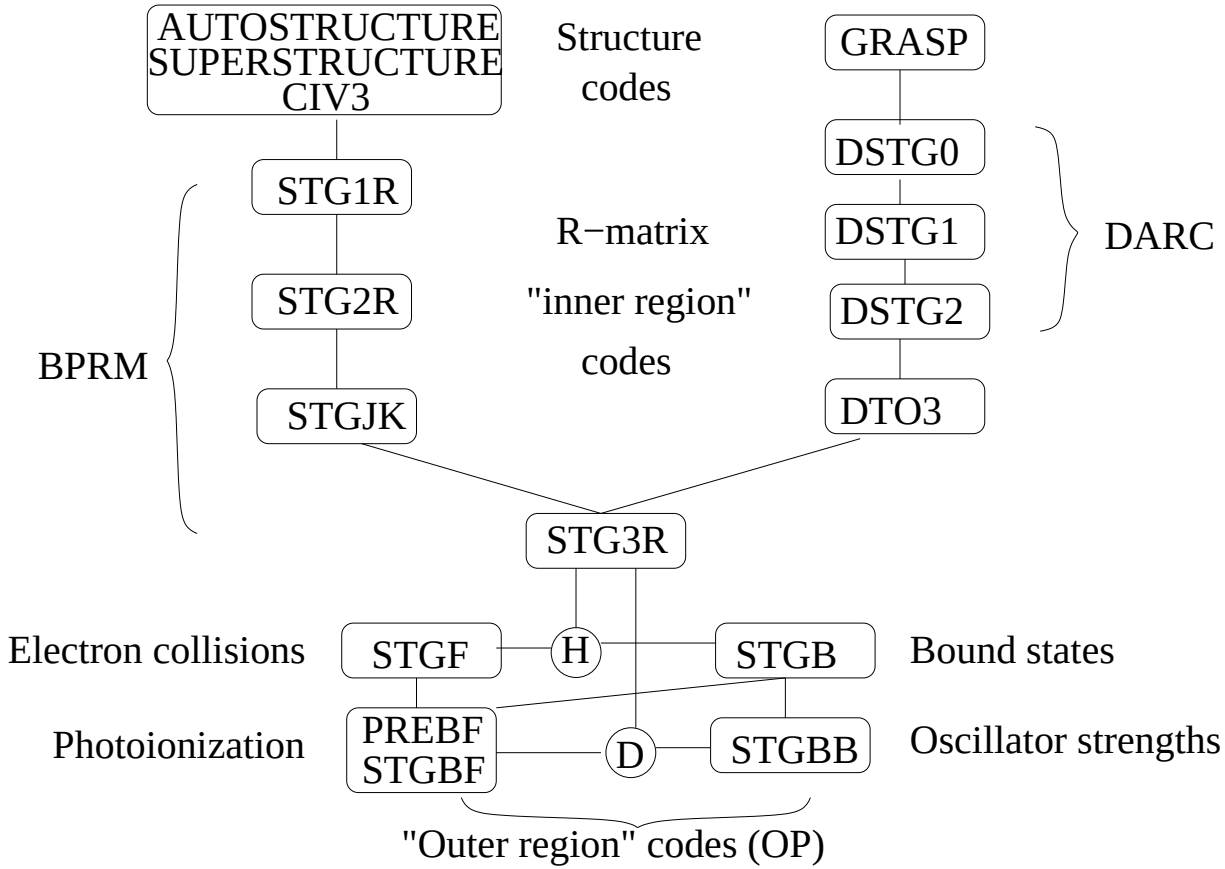

Practical implementation; code suite: `http://amdpp.phys.strath.ac.uk/UK_RmaX`

Parallel Classic R-matrix

- Parallel and serial Classic R-matrix codes are available at the UK RmaX website (userid: UK_RmaX password: H.DAT - only necessary for accessing parallel suite)
  http://amdpp.phys.strath.ac.uk/UK_RmaX/

- Contain many useful features developed over many years.

- Want to use on different parallel architectures: SMP & Beowulf clusters.

- Want to use on many systems: x86 clusters, Itanium Altix SMP, IBM SP, Cray X1E etc. i.e. portability is paramount.

Parallel Strategy

General philosophy: do as little message passing as possible — rather, compute same thing independently on each processor (degrades scaling, but then so does slow MPI). Maintain interchangeability of passing files with serial codes.

- PSTG1R: Distribute generation of bound-continuum and continuum-continuum integrals over a node (whole integrals).
- PSTG2R: Distribute clusters of symmetries over a node.
- PSTG3R, PSTG3NX: Use scaLAPACK (1.7) PDSYEVD to diagonalize a matrix distributed over many processors (NOT a distribution by symmetry — don't have enough memory).
- PSTGB: Distribute clusters of symmetries over a node.
- PSTGF, PSTGICF: Distribute by energy over many processors.

Application: RMPS

Recall,

$$\Psi = A \sum\!\!\!\!\!\!\int_{\nu} \psi_\nu \phi \, . \tag{39}$$

The R-matrix with pseudo-states approach (like CCC) replaces the sum over high Rydberg states and the integration over continuum states by a quadrature over Laguerre states.

The continuum basis plus Laguerre basis is over complete. The original RMPS implementation of Bartschat et al (1996) just Schmidt orthogonalized the two and discarded high-lying basis states. Badnell and Gorczyca (1997) diagonalize the matrix of overlaps to form the reduced linearly independent basis. The Buttle correction is also transformed appropriately, noting that the one-body Hamiltonian is no longer diagonal.

In fusion plasmas, visible-VUV spectroscopy of light neutral atoms and near neutral ions follows from excitation of $n = 3$ and $n = 4$ levels. These are strongly coupled to the continuum. All non-RMPS excitation data is suspect.

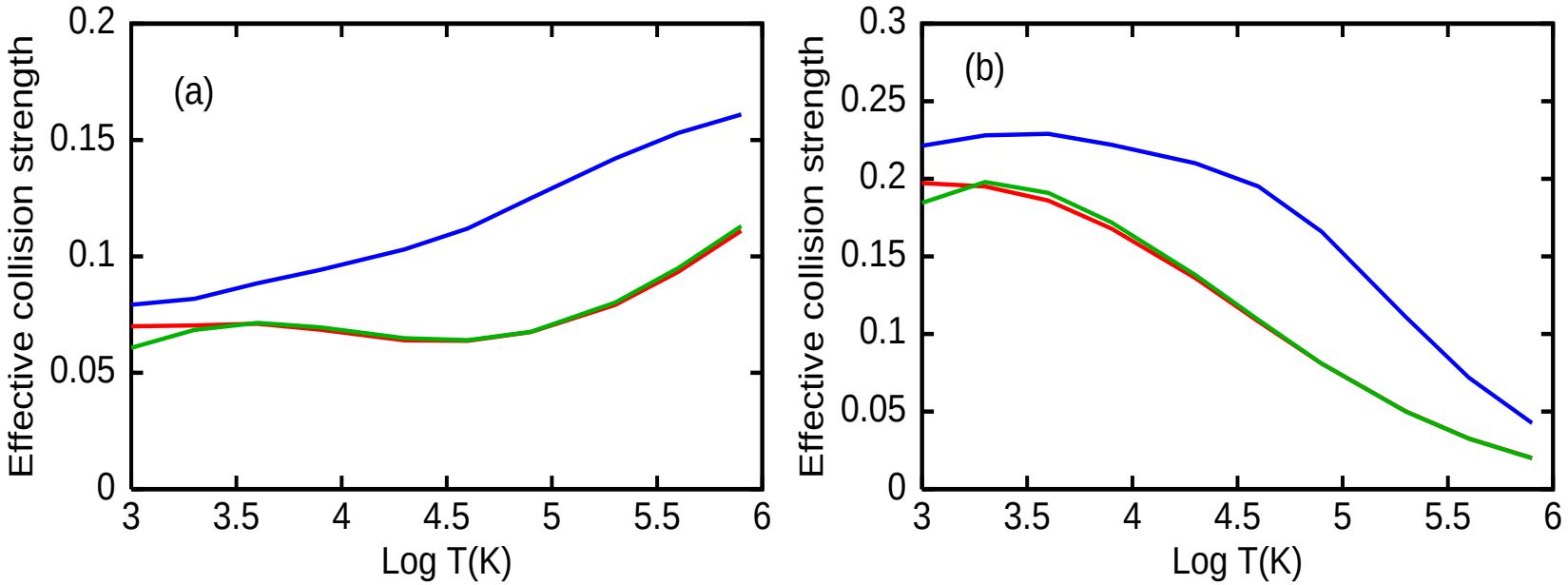

B^+: Effective collision strengths for excitation, from (a) the $2s^2\ ^1S$ ground term and (b) the $2s2p\ ^3P$ metastable term, to the $2s4s\ ^1S$ upper term. The blue curves are from the present 20CC R-matrix calculation, the red curves are from the present 114CC RMPS calculation, and the green curves are from the present 134CC RMPS calculation.

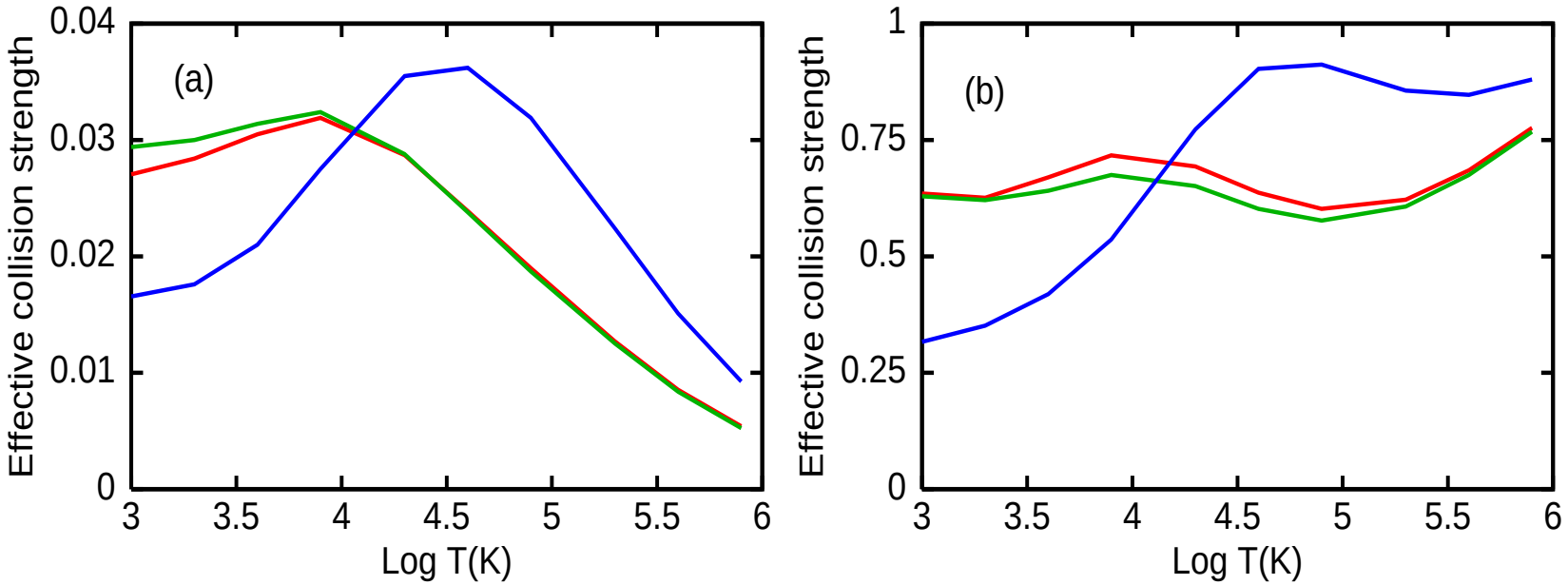

B^+: Effective collision strengths for excitation, from (a) the $2s^2\ ^1S$ ground term and (b) the $2s2p\ ^3P$ metastable term, to the $2s4f\ ^3F$ upper term. The blue curves are from the present 20CC R-matrix calculation, the red curves are from the present 114CC RMPS calculation, and the green curves are from the present 134CC RMPS calculation.

RMPS *adf04*

Maxwell-averaged upsilon files exist for:

- H-: H, He^{+}, Li^{2+}, Be^{3+}, B^{4+}, C^{5+}
- He-: He, Li^{+}, Be^{2+}
- Li-: Li, Be^{+}, B^{2+}, C^{3+}
- Be-: Be, B^{+}, C^{2+}
- B-: B

- Neutral Ne, BP, low energy only.

Badnell, Ballance, Griffin, Mitnik in a series of J.Phys.B papers.

MQDT/ICFT

Multi Channel Quantum defect Theory (MQDT):

$$K_{\rm oo} = \mathcal{K}_{\rm oo} - \mathcal{K}_{\rm oc}\left[\mathcal{K}_{\rm cc} - \tan(\pi\nu)\right]^{-1}\mathcal{K}_{\rm co}$$

$$S_{\rm oo} = \mathcal{S}_{\rm oo} - \mathcal{S}_{\rm oc}\left[\mathcal{S}_{\rm cc} - {\rm e}^{-2\pi{\rm i}\nu}\right]^{-1}\mathcal{S}_{\rm co}$$

$$D_{\rm o} = \mathcal{D}_{\rm o} - \mathcal{S}_{\rm oc}\left[\mathcal{S}_{\rm cc} - {\rm e}^{-2\pi{\rm i}\nu}\right]^{-1}\mathcal{D}_{\rm c}$$

- Applies to all closed-channels.
- Include long-range coupling potentials by retaining only the finite part of the divergent integrals (Gorczyca et al 1996).
- Intermediate Coupling Frame Transformation R-matrix approach (ICFT) then terms-couples the entire unphysical K- or S-matrix.

ICFT validation

Table 2. Rate coefficients for selected transitions in Fe^{14+} in units of 10^{-10} cm^3 s^{-1}, calculated using the four methods discussed in the text.

Transition	T (eV)	JAJOM	GFT	ICFT	Breit–Pauli
$3s^2\ {}^1S_0 \rightarrow 3s3p\ {}^3P_1$	30	2.05	2.67	5.47	5.65
$3s^2\ {}^1S_0 \rightarrow 3s3p\ {}^1P_1$	50	114	115	114	115
$3s3p\ {}^3P_2 \rightarrow 3s3p\ {}^1P_1$	15	2.69	2.68	9.72	9.55
$3s3p\ {}^3P_2 \rightarrow 3p^2\ {}^1D_2$	40	4.01	0.61	4.40	4.48

Griffin et al (1998)

- Resonance series converge on levels ICFT, GFT unlike JAJOM.
- Background is correct for ICFT, unlike JAJOM, GFT.

Ni^{4+}

Badnell and Griffin (1999)

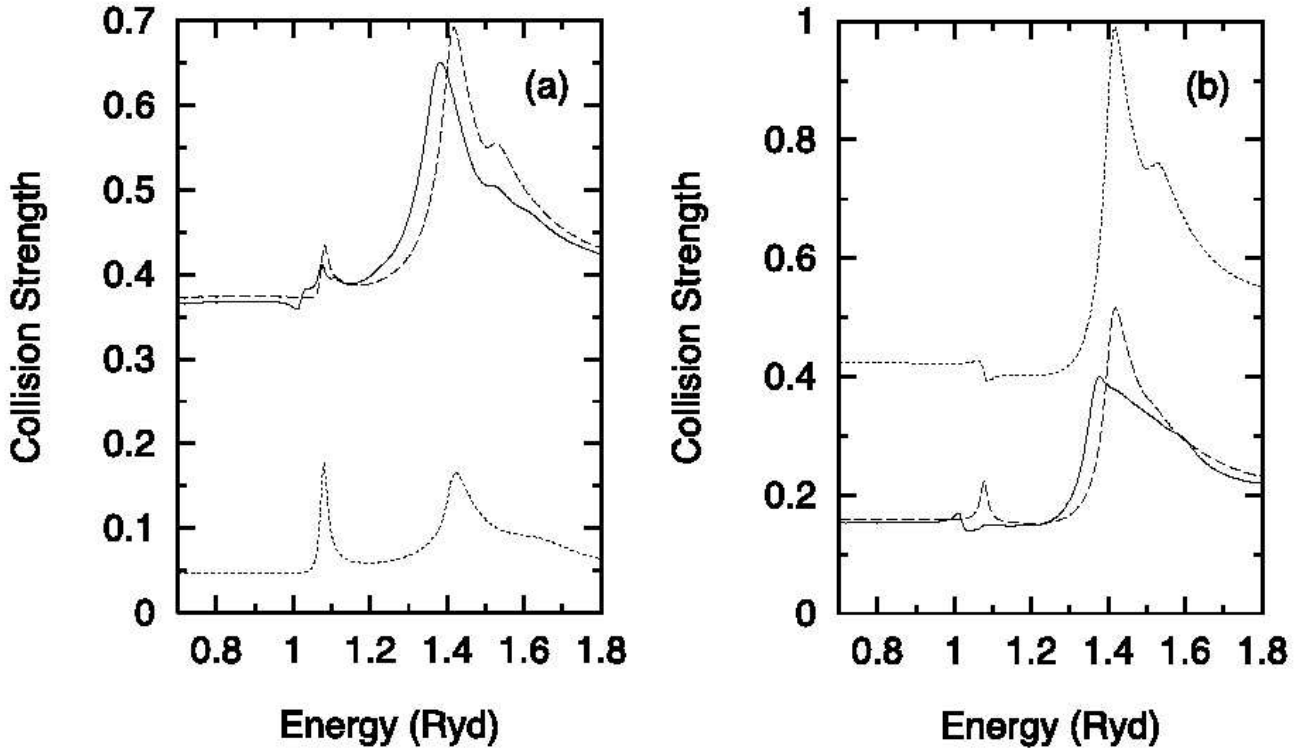

Figure 5. R-matrix electron-impact excitation collision strengths for the transitions (a) $^5D_4-^3H_4$ and (b) $^5D_4-^3F_4$ in Ni^{4+}. Full curve, Breit–Pauli; dashed curve, ICFT; dotted curve, jK-coupling.

- 'Correlation' resonances, which arise in $\mathcal{S}_{\rm oo}$, are well represented.

RM ICFT: along isoelectronic sequences

- Create a baseline database for electron-impact excitation which includes resonant enhancement: all ions of a sequence up to Zn (or Kr).
- Consider shell boundaries: H-, He-, Li- and F-, Ne-, Na-.
- Use (Perl) script to automate R-matrix calculation — requires reliable, robust codes.
- Works on serial or parallel machines.
- Uses AUTOSTRUCTURE (for structure and infinite energy limit points Bethe/Born) and ICFT R-matrix approach.
- End product: *adf04* file.
- R-matrix analysis package (RAP) has been developed by Mike Witthoeft (Python-based GUI) to validate the large amount of data.

- F-like sequence: see Witthoeft, Whiteford & Badnell J.Phys.B40, 2969 (2007).

- Na-like sequence:

  Outer-Shell: $(nl \rightarrow n'l')$ for $n, n' = 3-6$ — see Liang, Whiteford & Badnell Astron. Astrophys. 500, 1263 (2009)

  Inner-shell: 134CC $(2\mathrm{p}^6 3l, 2\mathrm{p}^5 3l3l',$ ex $3\mathrm{d}^2)$ allowing for Auger and radiation damping of resonances — Liang, Whiteford & Badnell J.Phys.B (At Press)

- Ne-like: 209CC $2\mathrm{s}^p 2\mathrm{p}^q nl\ (n = 2-5)$ and $2\mathrm{p}^2 2\mathrm{p}^5 n'l' (n' = 6, 7 \quad l' = 0-2)$ — Liang & Badnell (In progress)

- H-like and He-like sequences in ADAS — Witthoeft & Whiteford, methodology as per previously published for single ions (i.e. allows for radiation damping.)

- Li-like: simpler version of Na-like (TBD)

Example: F-like sequence

- $2s^2 2p^5, 2s2p^6, 2s^2 2p^4 3l, 2s2p^5 3l, 2s^2 2p^4 4l$: 87 terms and 195 levels.
- All ions from Ne^+ to Kr^{27+}.
- Structure automatically optimized for each individual ion.
- Good agreement of gf-values with Fawcett (1984).

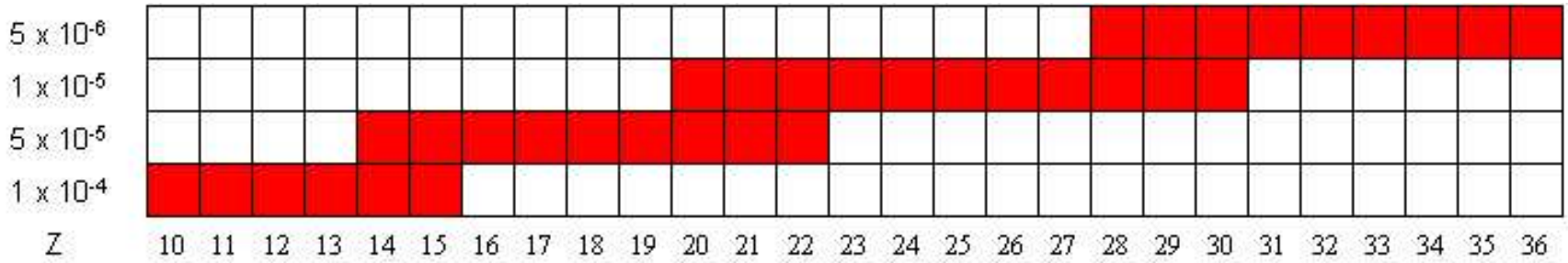

Energy meshes used for each ion - note overlaps as checks.

Energy mesh convergence

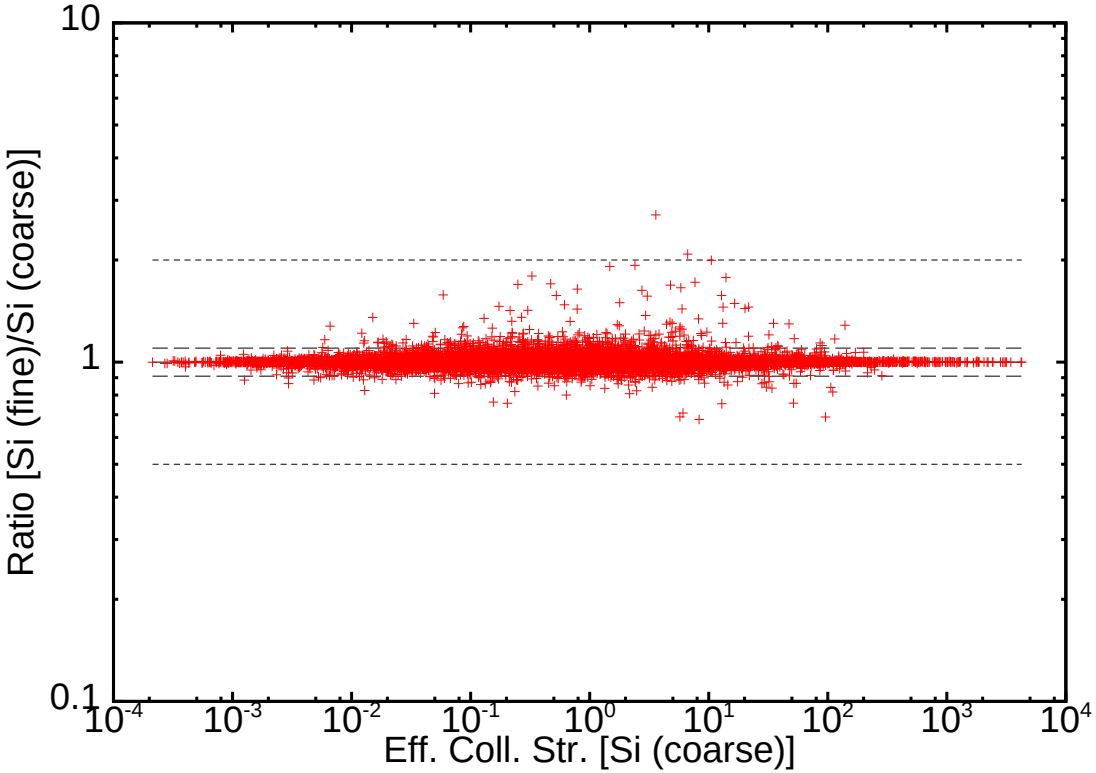

Si^{5+}, at 7.2×10^4K. Only 2.5% of transitions give rise to differences exceeding 10%.

Fine-structure transition

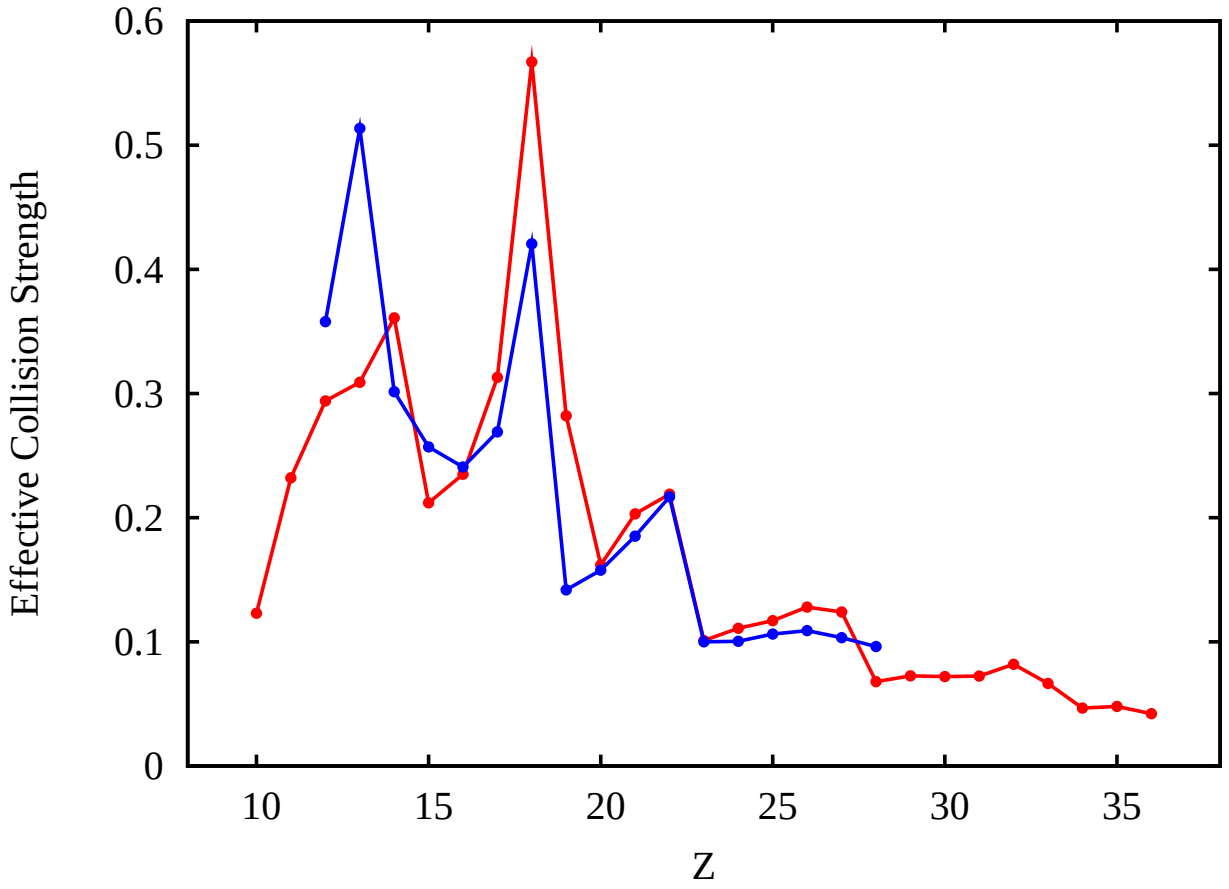

Red curve: ICFT-RM; blue curve: BPRM, Berrington et al (1998). $T = 10^3 z^2 \mathrm{K}$.

The march of the resonances

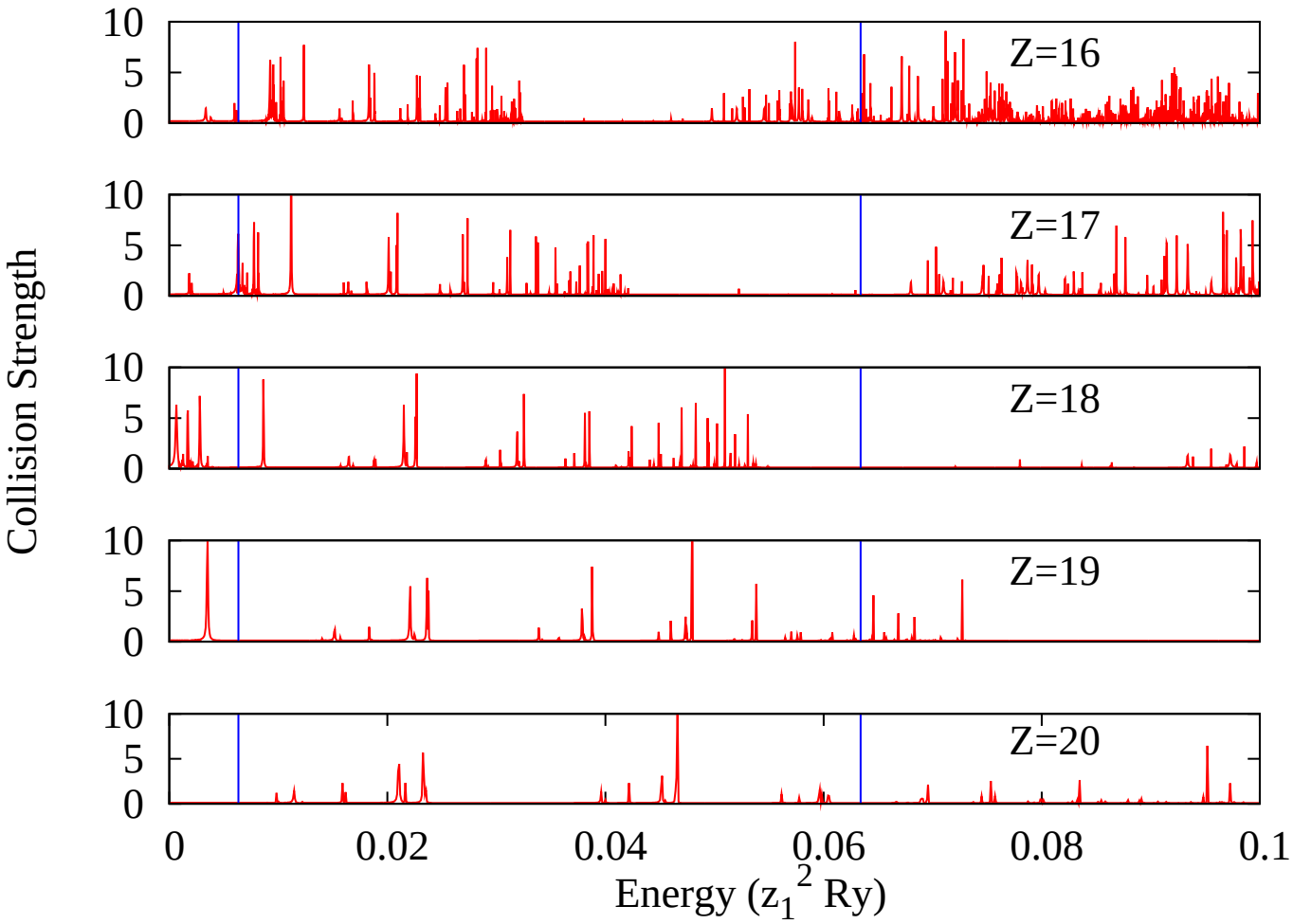

Fe^{17+}

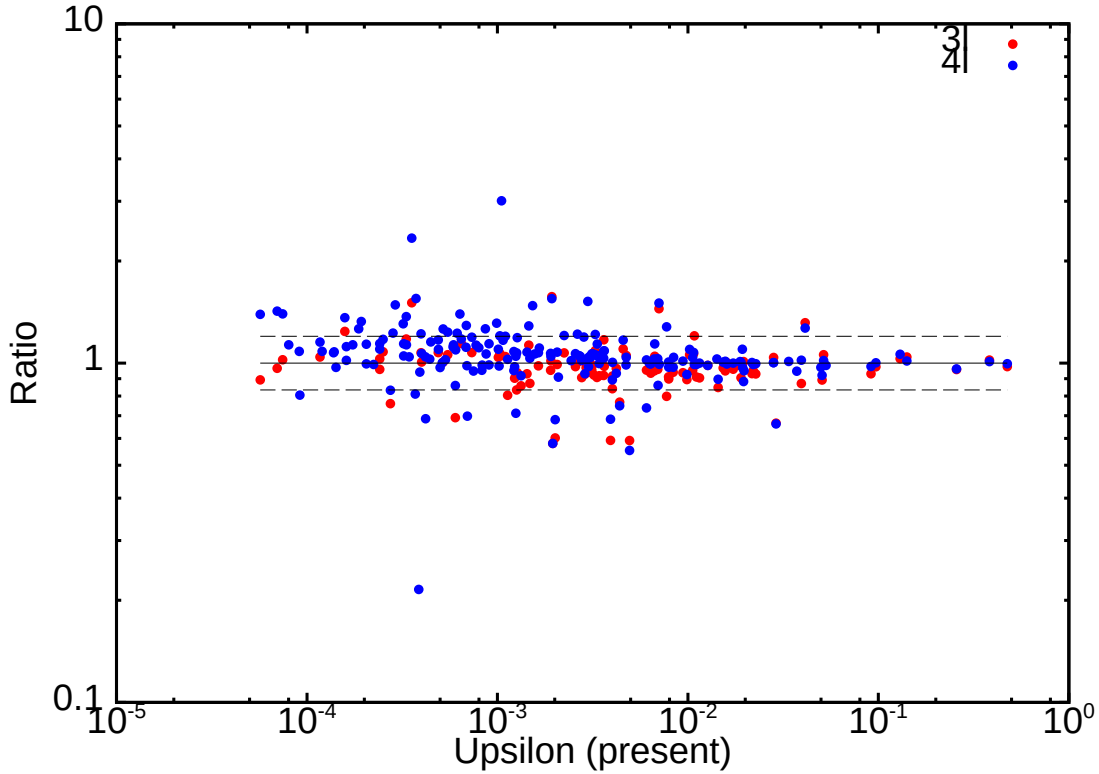

Comparison, for all transitions from the ground level, with previous results of Witthoeft et al (2006).

Dirac R-matrix for heavy species

Our preferred approach to electron-impact excitation for ADAS is R-matrix. Autoionizing levels are included implicitly by it rather than explicitly within the GCR modelling.

Main drawback is that R-matrix calculations are computationally demanding (impossible) for complex (i.e. heavy) species.

Semi-relativistic plane-wave Born (SR-PWB) excitation data from Cowan's code (CA and level-resolved) and AUTOSTRUCTURE (level-resolved only) provide complete 'baseline' coverage.

We have incorporated the Dirac R-matrix code within our parallel and radiation damped framework.

We compare the effect of using R-matrix as opposed to SR-PWB data on the resultant spectral signature of Ni-like Xe^{26+}, as an example, (Badnell et al 2004).

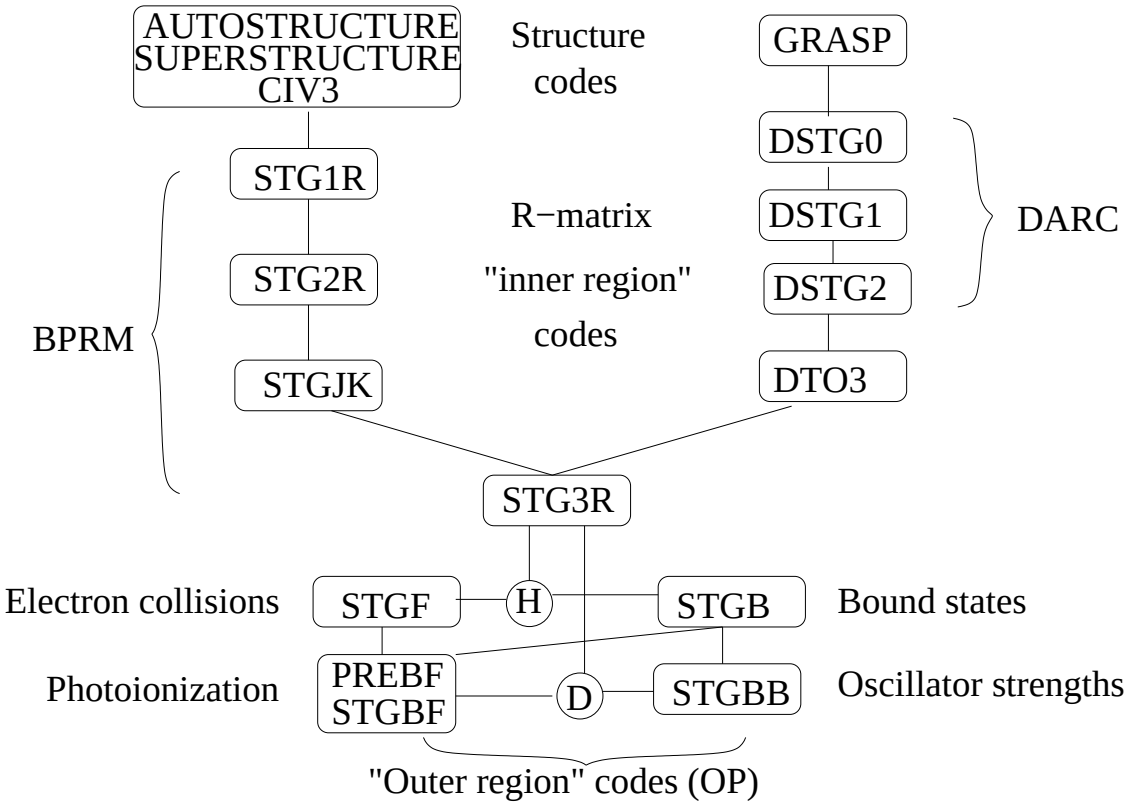

Flow diagram illustrating the interconnectivity between the Breit–Pauli, Dirac–Coulomb and Opacity Project (OP) R-matrix code suites.

Results of 129CC Dirac-Coulomb R-matrix calculation

$(3\mathrm{d}^{10}, 3\mathrm{d}^{9}nl, n = 4-5, l = 0 \text{ to } n-1.)$

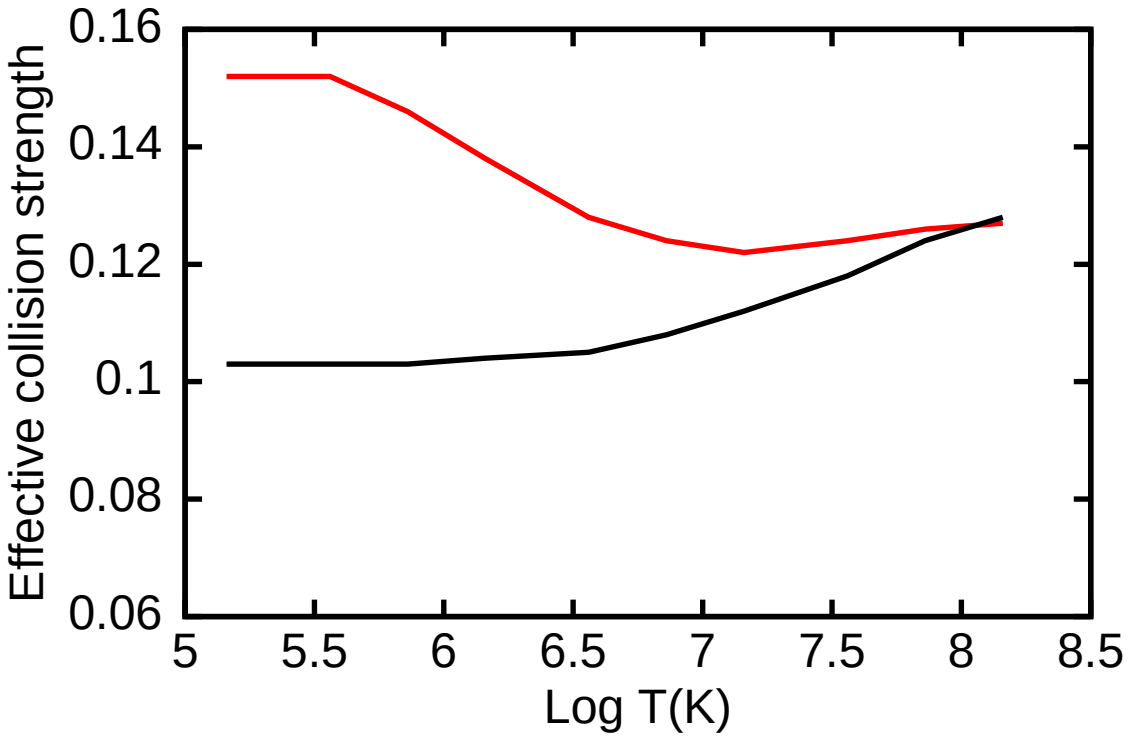

Effective collision strengths for the $3\mathrm{d}^{10}\ {}^1\mathrm{S}_0 - 4\mathrm{d}^1\mathrm{S}_0$ transition in Xe^{26+}:

Red curve, 129CC Dirac–Coulomb R-matrix; black curve, plane-wave Born (baseline data).

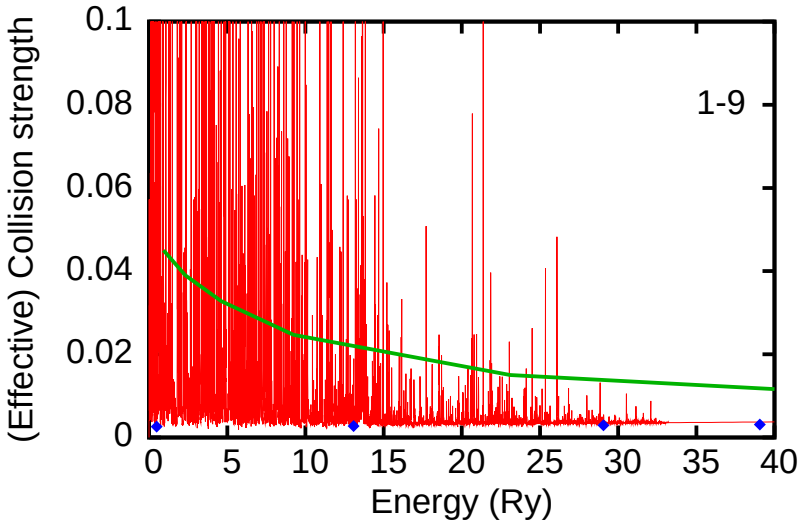

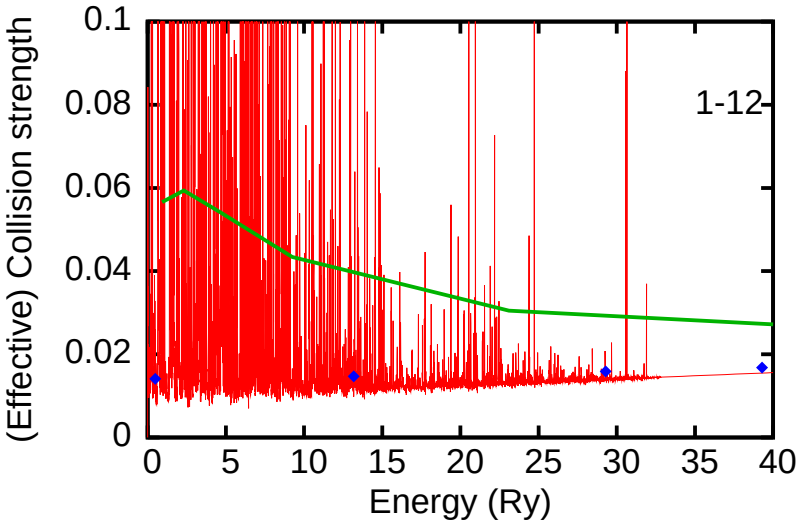

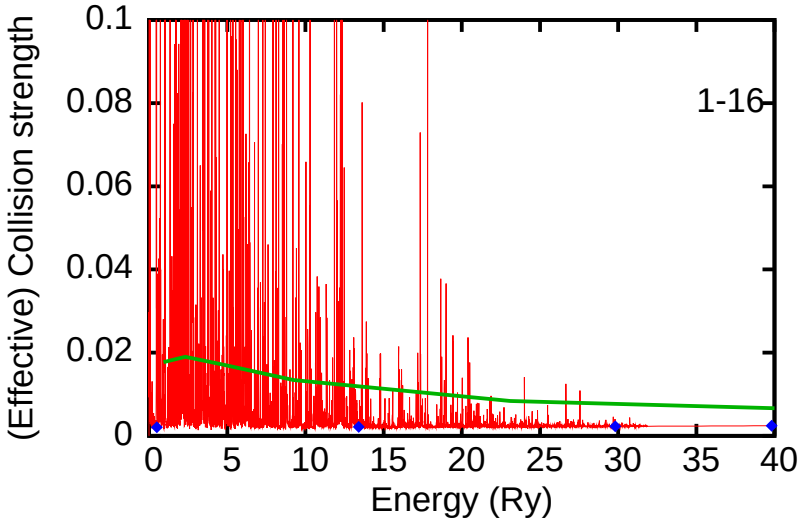

$3\mathrm{d}^{10} - 3\mathrm{d}^{9}4\mathrm{p}\ (J = 0 - 1)$

Diamonds, plane-wave Born collision strengths.

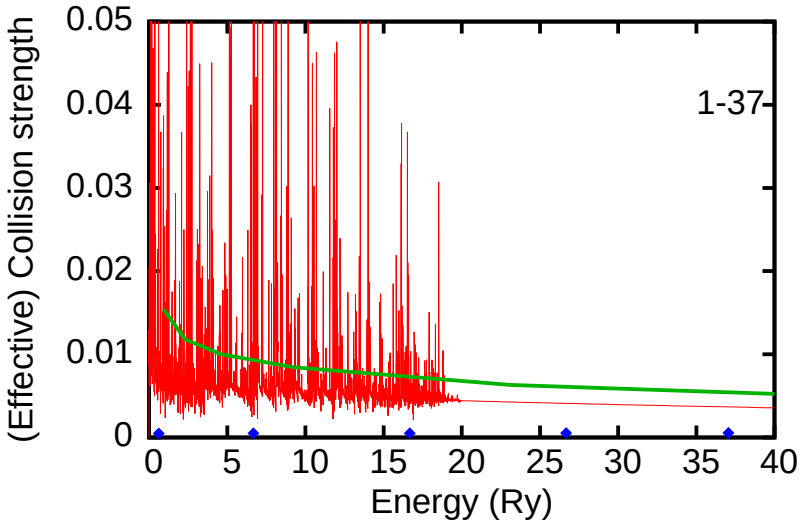

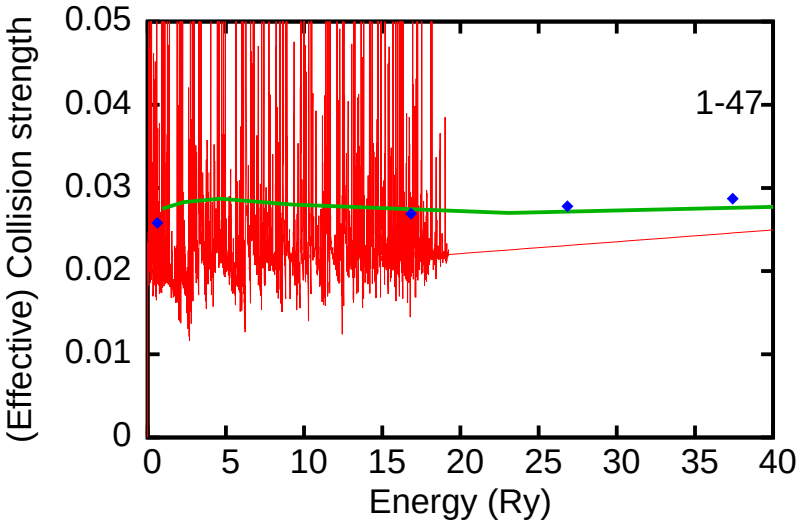

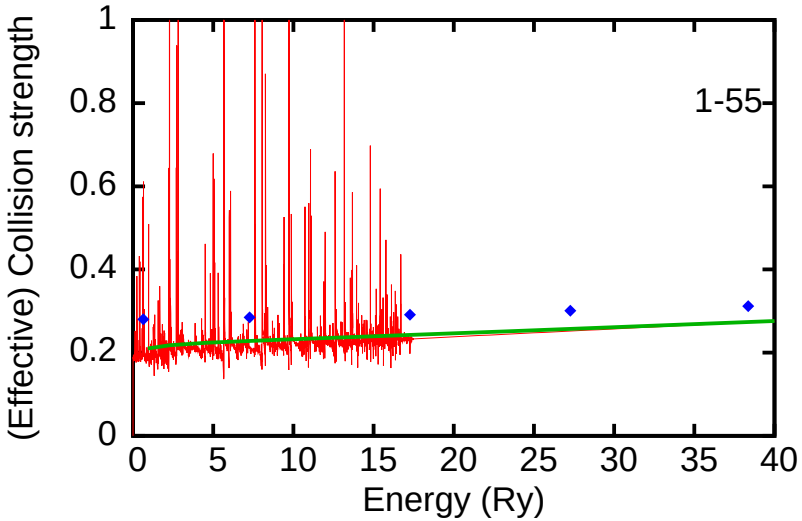

$3\mathrm{d}^{10} - 3\mathrm{d}^{9}4\mathrm{f}\ (J = 0 - 1)$

Diamonds, plane-wave Born collision strengths.

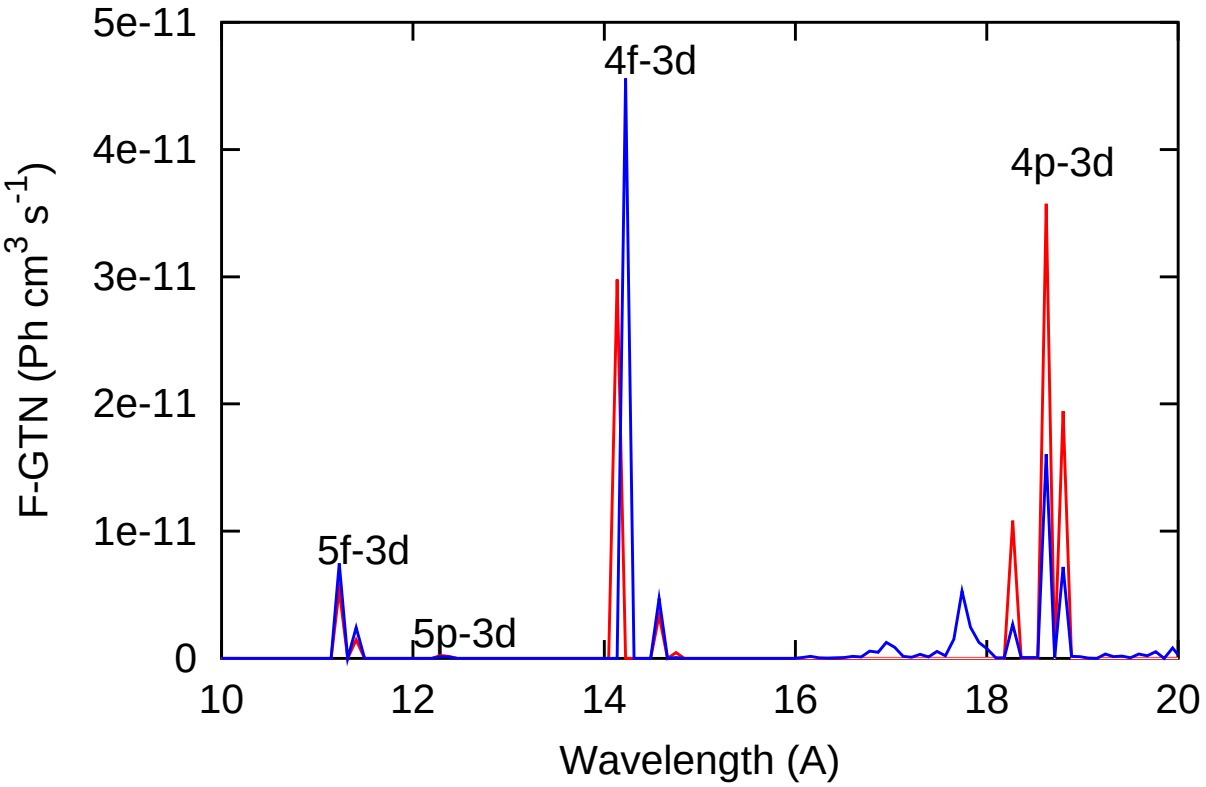

$\mathcal{F}$-$\mathcal{GTN} = (N^z/N_{\rm tot})|_{\rm eq}\mathcal{F}$-$\mathcal{PECC}^z$ for Xe^{q+} at $T_{\rm e} = 550$eV and $N_{\rm e} = 10^{13}$cm^{-3}: red curve, utilizing Dirac–Coulomb R-matrix excitation data; blue curve, utilizing plane-wave Born (baseline) excitation data; both for Xe^{26+} only. (The feature between 16–18 Å arises from other Xe ionization stages.)

Heavy Species - the future

- Stabilize parallel Dirac-Coulomb R-matrix codes —- dipole matrices. (Pretty much done.)
- Port QED/Breit interaction from GRASP to DARC $\Rightarrow$ Dirac-Breit R-matrix.
- Investigate fully-relativistic treatment for the 'outer region'.
- Dirac RMPS using L-spinors. (Done.)
- ICFTR: ICFT breaks down at $\gtrsim$ Kr $\Rightarrow$ use kappa-averaged relativistic wavefunctions.

Towards ICFTR

ICFT R-matrix method is less computationally demanding than BP/DARC.
$\Rightarrow$ Of interest to extend ICFT via using relativistic orbitals.

The ICR approach (in AUTOSTRUCTURE) averages the orbitals over kappa, neglects the small component (in general) and then carries-out the radial integrals required for the BP structure.

The relativistic analogue of integrals (RI) method takes fully relativistic radial integrals from GRASP and averages over kappa and feeds them back into the BP structure.

Some comparisons:

Energy levels (Ry) in W^{70+}. (From Jonauskas et al JPB v38 L79 (2005), +ICR.)

Index	Level	IC	HFR	DF	RI	ICR
1	2s2 1S0	-14472.2313	-14606.1630	-14661.2007	-14661.2127	-14660.1972
2	2s12p1 3P0	11.8033	9.5122	12.7642	13.3690	12.4027
3	2s12p1 3P1	14.4817	12.5698	15.6393	16.3163	15.4486
4	2p2 3P0	32.9833	29.5304	35.8501	36.6611	35.0358
5	2s12p1 3P2	101.4780	125.3516	123.2548	122.9797	123.2114
6	2s12p1 1P1	107.3621	131.9927	129.7459	129.3913	129.8507
7	2p2 3P1	119.6724	141.7643	142.9160	143.2261	142.6208
8	2p2 1D2	121.6674	143.8498	144.8975	145.2266	144.7094
9	2p2 3P2	210.3791	258.4229	254.3276	253.8651	254.5042
10	2p2 1S0	214.6380	262.8561	258.6676	258.1166	258.9496

Note, I obtain DF ground at -14660.2 with both uniform and Fermi charge nucleus.

Radiative decay of the U^{89+} $1s2s2p\ ^4P_{5/2}$ metastable level.

	$\Delta E(\mathrm{M1})$	$\Delta E(\mathrm{M2})$	$S(\mathrm{M1})$	$S(\mathrm{M2})$
IC	6972.7	7172.1	0.0255	0.00221
ICR	7075.5	7407.2	0.0632	0.00231
DF	7078.0	7409.9	0.0573	0.00236

ICR more elegant — more self-contained $\Rightarrow$ extend to ICFTR by coding for a BP R-matrix kappa=averaged relativistic continuum basis along the same lines.

Collaborators

Connor Ballance, Dario Mitnik & Don Griffin (Rollins)

Tom Gorczyca (Western Michigan)

Keith Berrington (Sheffield Hallam)

Guiyun Liang, Marin O Mullane, Mike Witthoeft, Allan Whiteford & Hugh Summers (Strathclyde)

Patrick Norrington (QUB)